Waves on a long string with side branches

R. Porter

May 21, 2018

Abstract

We consider the effect of finite length strings branched from an infinite string on the waves propagating along that string. Alternative physical settings of the problem could involve transmission-line problems in electromagnetism, narrow-channel propagation in acoustics or water waves or quantum graphs. It is shown that waves are totally reflected at frequencies which coincide with resonance on any branched string. As a consequence, a multiple branches of tapered length can be used to manufacture a broadbanded stop filter. This has close connections to a phenomenon referred to as 'rainbow trapping' in Physics.

1 Introduction

This problem arose as a possible means of developing an understanding to the solution of a more complicated problem in acoustics (Jan & Porter (2018, in preparation)), specifically the reflection of waves propagating in a finite-width waveguide from multiple narrow channels extending perpendicular to one of the two parallel waveguide walls. The current problem is applicable to the situation where long waves propagate in narrow waveguides with equally narrow side channels and wave propagation in both the waveguide and side channels is assumed, to leading order, one dimensional.

It's not yet clear that the solution contained within this report helps directly with the specific issues being addressed in Jan & Porter (2018). Nevertheless, the solution does contain some interesting mathematical features and results which do not, by themselves, merit journal publication but may be useful to researchers interested in topics related to what has become known as 'rainbow trapping'.

2 Wave reflection from a single branch

Consider an infinitely long uniform string under tension aligned with the x-axis. At $x = x_n$, the string is connected to an equal string of finite length $2c_n$ under equal load which runs perpendicular to the x-axis from $(x_n, -c_n)$ to (x_n, c_n). We assume time harmonic motions of angular frequency ω. Then the equation governing the string displacement $\Re\{\eta(x)\mathrm{e}^{-\mathrm{i}\omega t}\}$ for $x < x_n$ and $x > x_n$ is

$$\eta''(x) + k^2\eta(x) = 0 \tag{1}$$

where $k^2 = \omega^2/c^2$ and $c^2 = T/\rho$ in terms of the tension, T, and the mass per unit length of the string, ρ.

The displacement for $0 < y < c_n$ along the positive half of the branch is given by $\Re\{\zeta_n(y)\mathrm{e}^{-\mathrm{i}\omega t}\}$, symmetry dictating that $\zeta_n(-y) = \zeta_n(y)$, where

$$\zeta_n''(y) + k^2\zeta_n(y) = 0, \qquad 0 < y < c_n \tag{2}$$

and we impose $\zeta_n'(c_n) = 0$ on account of the physical problem which motivated this study; a Dirichlet condition is more applicable for real strings. At the junction, displacements must match, implying that

$$\eta(x_n^-) = \eta(x_n^+) = \zeta_n(0^+) \tag{3}$$

and the vertical forces must balance so that

$$\eta'(x_n^+) + 2\zeta_n'(0^+) = \eta'(x_n^-). \tag{4}$$

In $x < x_n$, the solution is

$$\eta(x) = A_n^-\mathrm{e}^{\mathrm{i}kx} + B_n^-\mathrm{e}^{-\mathrm{i}kx} \tag{5}$$

and in $x > x_n$,

$$\eta(x) = A_n^+\mathrm{e}^{\mathrm{i}kx} + B_n^+\mathrm{e}^{-\mathrm{i}kx} \tag{6}$$

whilst along the branch

$$\zeta_n(y) = D_n \cos k(c_n - y). \tag{7}$$

Imposing the conditions at $x = x_n$ gives

$$A_n^-\mathrm{e}^{\mathrm{i}kx_n} + B_n^-\mathrm{e}^{-\mathrm{i}kx_n} = A_n^+\mathrm{e}^{\mathrm{i}kx_n} + B_n^+\mathrm{e}^{-\mathrm{i}kx_n} = D_n \cos kc_n \tag{8}$$

and

$$A_n^+\mathrm{e}^{\mathrm{i}kx_n} - B_n^+\mathrm{e}^{-\mathrm{i}kx_n} - 2\mathrm{i}D_n \sin kc_n = A_n^-\mathrm{e}^{\mathrm{i}kx_n} - B_n^-\mathrm{e}^{-\mathrm{i}kx_n}. \tag{9}$$

Eliminating D_n gives

$$A_n^+\mathrm{e}^{2\mathrm{i}kx_n} - B_n^+ - 2\mathrm{i}\tan kc_n\{A_n^+\mathrm{e}^{2\mathrm{i}kx_n} + B_n^+\} = A_n^-\mathrm{e}^{2\mathrm{i}kx_n} - B_n^- \tag{10}$$

which forms a pair of equations, together with

$$A_n^-\mathrm{e}^{2\mathrm{i}kx_n} + B_n^- = A_n^+\mathrm{e}^{2\mathrm{i}kx_n} + B_n^+, \tag{11}$$

for the four amplitudes present on the infinite string.

We can either assume that the incoming wave amplitudes A_n^-, B_n^+ are given and determine the outgoing wave amplitudes B_n^-, A_n^+ (the scattering matrix approach); or that the wave amplitudes to the left of the junction A_n^-, B_n^- are prescribed and determine wave amplitudes A_n^+, B_n^+ to the right (the transfer matrix approach.)

Consider the first of these. Then we find from (10), (11)

$$\begin{pmatrix} A_n^+ \\ B_n^- \end{pmatrix} = \mathsf{S}(x_n)\begin{pmatrix} A_n^- \\ B_n^+ \end{pmatrix}, \tag{12}$$

where

$$\mathsf{S}(x_n) = \mathrm{e}^{\mathrm{i}kc_n}\begin{pmatrix} \cos kc_n & \mathrm{i}\sin kc_n\mathrm{e}^{-2\mathrm{i}kx_n} \\ \mathrm{i}\sin kc_n\mathrm{e}^{2\mathrm{i}kx_n} & \cos kc_n \end{pmatrix}. \tag{13}$$

We note, in passing, that $\det\{\mathsf{S}(x_n)\} = 1$ and $\mathsf{S}^{-1}(x_n) = \mathsf{S}^*(-x_n)$ which encodes directional invariance.

For example, if $A_n^- = 1$ and $B_n^+ = 0$ and we let $B_n^- = R$ and $A_n^+ = T$ be reflection and transmission coefficients then

$$T = \mathrm{e}^{\mathrm{i}kc_n} \cos kc_n, \qquad R = \mathrm{i}\mathrm{e}^{2\mathrm{i}kx_n} \mathrm{e}^{\mathrm{i}kc_n} \sin kc_n \tag{14}$$

and we see that $|R|^2 + |T|^2 = 1$. Of special note is $kc_n \to \frac{1}{2}\pi$, which corresponds to resonance in the branch with a node at $y = 0$ and an anti-node at $y = c_n$. Here, $T = 0$, $R = -\mathrm{e}^{2\mathrm{i}kx_n}$ and all wave energy is reflected. Note also that $kc_n = \pi$ is also a resonance with anti-nodes at both ends of the finite string. This gives rise to $R = 0$, $T = 1$ and the branch is transparent to (and a slave to) the waves on the infinite string. Hereafter we use the term "resonant" to refer to the former case where the displacement is zero at the junction and there is an anti-node at the ends of the branch.

The transfer matrix approach involves us arranging the original pair of equations (10), (11) for the four wave amplitudes as

$$\begin{pmatrix} A_n^+ \\ B_n^+ \end{pmatrix} = \mathsf{P}(x_n) \begin{pmatrix} A_n^- \\ B_n^- \end{pmatrix}, \tag{15}$$

where we find that

$$\mathsf{P}(x_n) = \begin{pmatrix} \mathrm{e}^{-\mathrm{i}kx_n} & 0 \\ 0 & \mathrm{e}^{\mathrm{i}kx_n} \end{pmatrix} \begin{pmatrix} 1 + \mathrm{i}t_n & \mathrm{i}t_n \\ -\mathrm{i}t_n & 1 - \mathrm{i}t_n \end{pmatrix} \begin{pmatrix} \mathrm{e}^{\mathrm{i}kx_n} & 0 \\ 0 & \mathrm{e}^{-\mathrm{i}kx_n} \end{pmatrix}. \tag{16}$$

where $t_n \equiv \tan kc_n$.

Again we see that $\det\{\mathsf{P}(x_n)\} = 1$ and $\mathsf{P}^{-1}(x_n) = \mathsf{P}^*(-x_n)$ and can recover the previous evaluation of R and T by inserting the appropriate substitutions for the wave amplitudes.

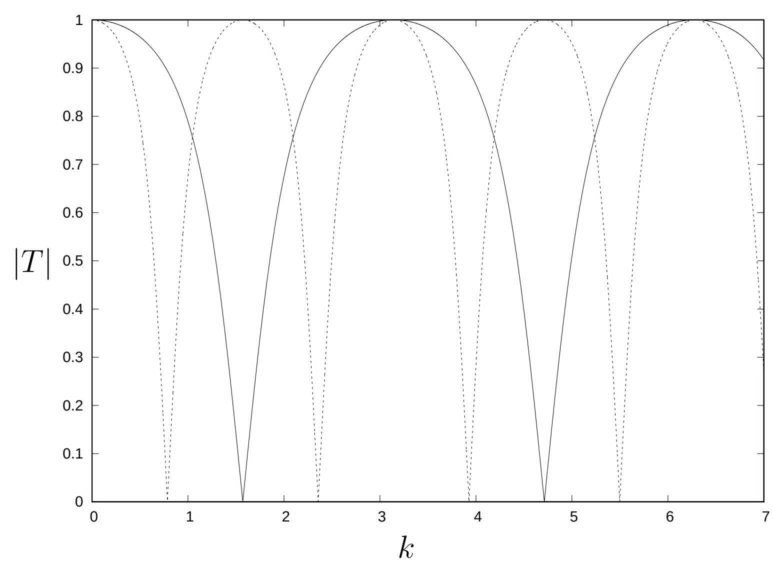

Figure 1: Modulus of transmission coefficient against k for a branch of length $c_1 = 1$ (solid) and $c_1 = 2$ (dashed).

In Fig. 1 we show the effect of a single branch. There is only one dimensionless number here, kc_1, and so the two curves of $c_1 = 1$ and $c_1 = 2$ are identical, but for a rescaling of k. Indeed, all we are plotting is the curve $|\cos kc_1|$ and we obviously confirm that total transmission occurs at $kc_1 = \pi$ and zero transmission at $kc_1 = \pi/2$.

3 Multiple branches

Consider now N branches placed along the string at $x = x_n$ for $1 \le n \le N$. We note that

$$\begin{pmatrix} A^-_{n+1} \\ B^-_{n+1} \end{pmatrix} = \begin{pmatrix} A^+_n \\ B^+_n \end{pmatrix} = \mathsf{P}(x_n)\mathsf{P}(x_{n-1})\ldots\mathsf{P}(x_1)\begin{pmatrix} A^-_1 \\ B^-_1 \end{pmatrix}. \tag{17}$$

We define an auxiliary node $x_0 = 0$ and can write (17) as

$$\begin{pmatrix} A^+_n \mathrm{e}^{\mathrm{i}kx_n} \\ B^+_n \mathrm{e}^{-\mathrm{i}kx_n} \end{pmatrix} = \mathbb{Q}_n \begin{pmatrix} A^-_1 \\ B^-_1 \end{pmatrix} \qquad \text{where} \qquad \mathbb{Q}_n = \mathsf{Q}_n\mathsf{Q}_{n-1}\ldots\mathsf{Q}_1 \tag{18}$$

where

$$\mathsf{Q}_n = \begin{pmatrix} 1+t_n & \mathrm{i}t_n \\ -\mathrm{i}t_n & 1-\mathrm{i}t_n \end{pmatrix}\begin{pmatrix} \mathrm{e}^{\mathrm{i}k\delta_n} & 0 \\ 0 & \mathrm{e}^{-\mathrm{i}k\delta_n} \end{pmatrix} \tag{19}$$

and $\delta_n = x_n - x_{n-1}$. Thus Q_n are also transfer matrices which only rely on the relative distance between neighbouring junctions on the string. On account of the particular structure of the matrices Q_n we can write

$$\mathbb{Q}_n = \begin{pmatrix} \beta_n & \gamma_n \\ \gamma^*_n & \beta^*_n \end{pmatrix} \tag{20}$$

where the asterisk denotes complex conjugate. The entries of $\mathbb{Q}_n$ are determined from the coupled recurrence relation

$$\left.\begin{aligned} \beta_n &= (1+\mathrm{i}t_n)\mathrm{e}^{\mathrm{i}k\delta_n}\beta_{n-1} + \mathrm{i}t_n\mathrm{e}^{-\mathrm{i}k\delta_n}\gamma^*_{n-1} \\ \gamma_n &= (1+\mathrm{i}t_n)\mathrm{e}^{\mathrm{i}k\delta_n}\gamma_{n-1} + \mathrm{i}t_n\mathrm{e}^{-\mathrm{i}k\delta_n}\beta^*_{n-1} \end{aligned}\right\} \qquad n = 2, 3, \ldots \tag{21}$$

with $\beta_1 = (1+\mathrm{i}t_1)\mathrm{e}^{\mathrm{i}k\delta_1}$, $\gamma_1 = \mathrm{i}t_1\mathrm{e}^{-\mathrm{i}k\delta_1}$.

To determine the overall scattering by N branches we use (18) with $n = N$ and let $A^-_1 = 1$, $B^+_N = 0$ such that $T = A^+_N$ and $R = B^-_1$ are reflection and transmission coefficients. Then the above can be written

$$\begin{pmatrix} T\mathrm{e}^{\mathrm{i}kx_N} \\ 0 \end{pmatrix} = \mathbb{Q}_N \begin{pmatrix} 1 \\ R \end{pmatrix} \tag{22}$$

from which we deduce

$$R = \gamma^*_N/\beta^*_N, \qquad T = \mathrm{e}^{-\mathrm{i}kx_N}(\beta_N + R\gamma_N). \tag{23}$$

Since $\mathbb{Q}_N$ is a product of transfer matrices, its determinant is equal to one and it follows that $T = \mathrm{e}^{-\mathrm{i}kx_N}/\beta^*_N$.

Under the current variables, amplitudes along each branch may be expressed, using (8), (18), (20) as

$$D_n = \sec kc_n(\beta_n + \gamma^*_n + R(\beta^*_n + \gamma_n)). \tag{24}$$

We consider the case where $\cos kc_n = 0$ in the next subsection.

In Fig. 2 the we show the effect of two branches on the transmission coefficient and note that $T = 0$ when there is node/anti-node resonance on either of the two strings (e.g. at $k = \frac{1}{4}\pi$, $\frac{1}{2}\pi$, $\frac{3}{4}\pi$ and total transmission when there is the coincidence of anti-node/anti-node resonance (e.g. at $k = \pi$). The four different curves show the effect of spacing between the branches which varies from $\delta_2 \equiv \delta = 0.8$ to $\delta = 0.1$.

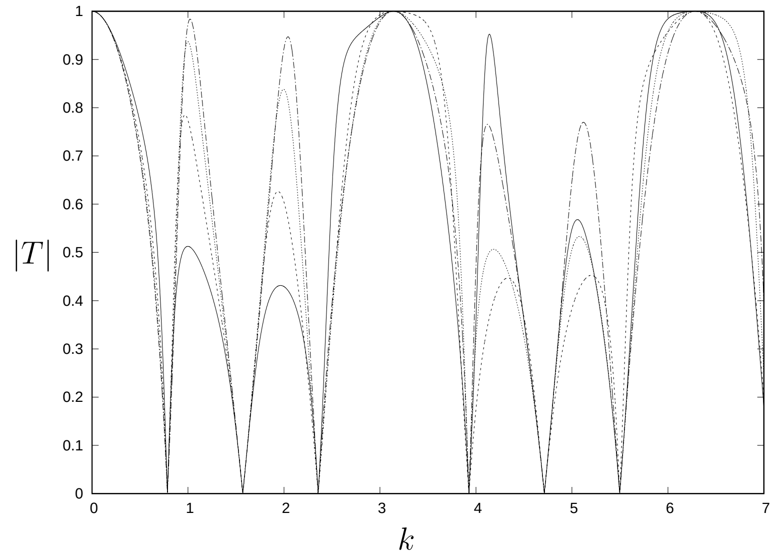

Figure 2: Modulus of transmission coefficient against k for two branches of lengths $c_1 = 1$ and $c_2 = 2$. The separation varies from $\delta = 0.8$ (solid), $\delta = 0.4$ (dashed), $\delta = 0.2$, (dotted), $\delta = 0.1$ (chained).

3.1 Branch resonance implies total reflection

Previously we showed that total reflection occurs when a single branch is made from the string such that the branch is resonant ($kc_n = \frac{1}{2}\pi$). Furthermore, Fig. 2 indicates that total reflection occurs when the frequency coincides with either of two branch resonances. So we turn our attention to investigating the effect of branch resonance on reflection.

Consider now an array of N branches of length c_n, $n = 1, 2, \ldots, N$ in a situation in which there exists an m such that $kc_m = \frac{1}{2}\pi$ and that m is the smallest value of n for which this holds. It follows from (3), (7) that $\eta(x_m^-) = 0 = \eta(x_m^+)$ and this implies from (8)

$$A_m^+ = -\mathrm{e}^{-2\mathrm{i}kx_m} B_m^+. \tag{25}$$

Implementing the transfer matrix approach over branches $n = 1, \ldots, m$ and using (25) in (18)

$$B_m^+ \begin{pmatrix} \mathrm{e}^{\mathrm{i}kx_m} & 0 \\ 0 & \mathrm{e}^{-\mathrm{i}kx_m} \end{pmatrix} \begin{pmatrix} -\mathrm{e}^{-2\mathrm{i}kx_m} \\ 1 \end{pmatrix} = \mathbb{Q}_m \begin{pmatrix} A_1^- \\ B_1^- \end{pmatrix} \equiv \begin{pmatrix} \beta_m & \gamma_m \\ \gamma_m^* & \beta_m^* \end{pmatrix} \begin{pmatrix} 1 \\ R \end{pmatrix}, \tag{26}$$

assuming an incident wave from the left with reflection coefficient R as before. Since determinants of transfer matrices are unity

$$\begin{pmatrix} 1 \\ R \end{pmatrix} = B_m^+ \mathrm{e}^{-\mathrm{i}kx_m} \begin{pmatrix} \beta_m^* & -\gamma_m \\ -\gamma_m^* & \beta_m \end{pmatrix} \begin{pmatrix} -1 \\ 1 \end{pmatrix} \tag{27}$$

and this implies

$$R = -\frac{\gamma_m^* + \beta_m}{\gamma_m + \beta_m^*} \tag{28}$$

revealing that $|R| = 1$. Thus we have shown that branch resonance, wherever it occurs in the array, implies total reflection.

We see that the earlier formula for D_m with $kc_m = \frac{1}{2}\pi$ should be interpreted as a 'zero-over-zero' limit (it ought to be possible to derive the value of this limit explicitly.)

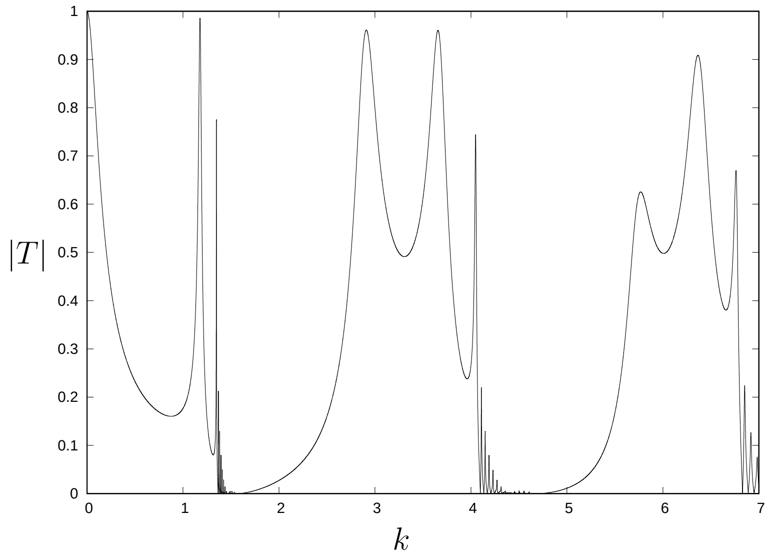

Figure 3: Modulus of transmission coefficient against k for $N = 16$ branches of lengths $c_n = 1 + 0.01(n-1)$, $n = 1, 2, \ldots, N$ with an equal separation $\delta = 0.01$ between branches.

Note finally that the proof above does not say anything about the solution beyond the mth branch. From the transfer matrix approach, we have, for $m+1 \le n \le N$

$$\begin{pmatrix} \mathrm{e}^{\mathrm{i}kx_N} A_N^+ \\ \mathrm{e}^{-\mathrm{i}kx_N} B_N^+ \end{pmatrix} = \mathsf{Q}_N \ldots \mathsf{Q}_n \begin{pmatrix} \mathrm{e}^{-\mathrm{i}kx_n} A_n^- \\ \mathrm{e}^{\mathrm{i}kx_n} B_n^- \end{pmatrix} \tag{29}$$

and since $|R| = 1$, we have $0 = T = A_N^+$, $B_N^+ = 0$ and so we infer that $A_n^- = B_n^- = 0$ for all $n > m+1$. This feature of the solution beyond the resonant branch is evident in Figs. 10–12.

In Fig. 3 we show $|T|$ for 16 branches which have a fixed separation $\delta = 0.01$ and whose length is tapered linearly with distance along the main string. That is, we define the length of the nth branch to be $c_n = 1 + 0.01(n-1)$. Thus $c_1 = 1$, $c_{16} = 1.15$ and the individual string resonances lie at discrete wavenumbers defined by $k = \frac{1}{2}\pi/c_n$. In Fig. 4 we magnify the region between the first branch resonance $k = \frac{1}{2}\pi/1.15 \approx 1.366$ and the last $k = \frac{1}{2}\pi$. From the analysis above we know that $|T| = 0$ at each of the 16 branch resonances and for frequencies in between there is some oscillatory behaviour in $|T|$; closer inspection reveals the peaks are smooth and do not extend to $|T| = 1$. Smaller scale peaks closer to $\frac{1}{2}\pi$, not visible on the scale of the plot in Fig. 4, are also present.

Figs. 5 and the magnified Fig. 6 show the same as before but for a separation of $\delta = 0.1$ instead of $\delta = 0.01$. There are more complicated multiple-scattering effects (in which N and δ control the frequency of oscillations to $|T|$) as well as branch resonance effects.

In Fig. 7 we have $N = 101$ branches defined as $c_n = 1 + 0.01(n-1)$, $\delta = 0.01$ between $c_1 = 1$ and $c_{101} = 2$. The branch resonances now occur over the range $\frac{1}{4}\pi < k < \frac{1}{2}\pi$. Without magnifying detail (the plot resolution is already 200000 points) the distribution of zeros of transmission over the range of branch-resonant frequencies form a broadbanded stop filter on the string. This exemplifies what physicists have called 'Rainbow Trapping'.

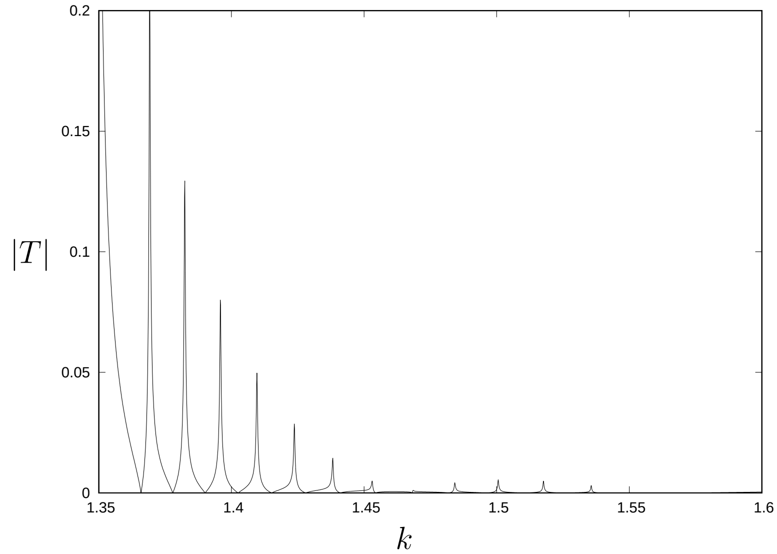

Figure 4: Magnification of Fig. 3 around branch resonances.

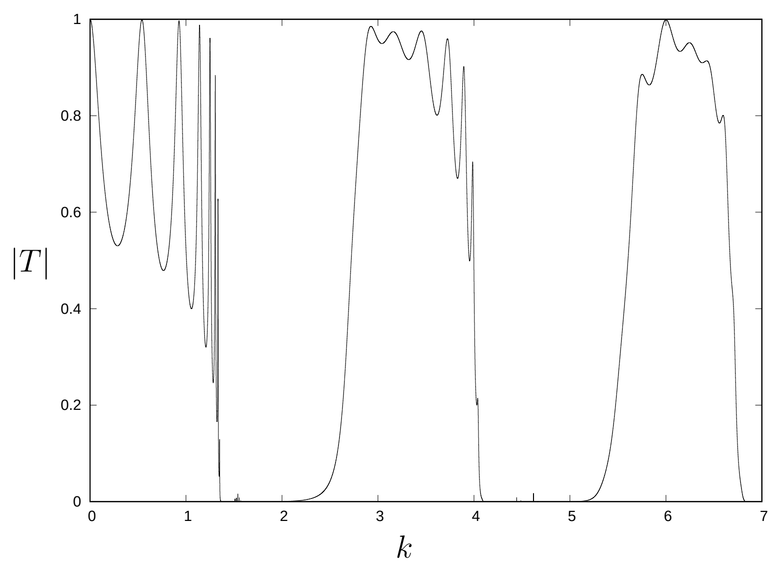

Figure 5: Modulus of transmission coefficient against k for $N = 16$ branches of lengths $c_n = 1 + 0.01(n-1)$, $n = 1, 2, \ldots, N$ with a separation $\delta = 0.1$ between branches.

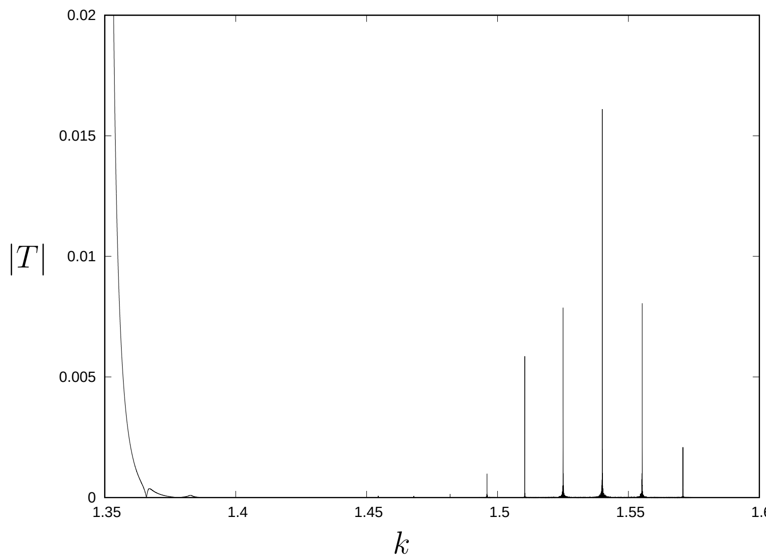

Figure 6: Magnification of Fig. 5 around branch resonances.

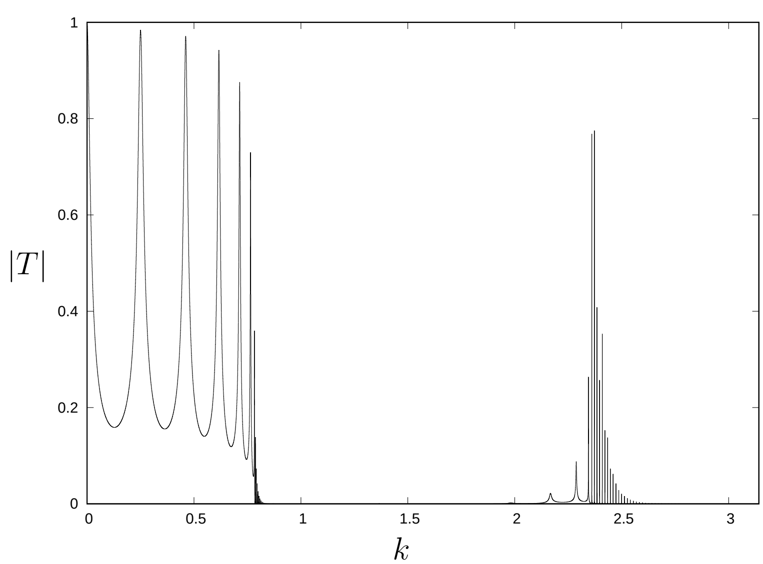

Figure 7: $|T|$ against k for $N = 101$ branches at $c_n = 1 + 0.01(n-1)$ and $\delta = 0.01$.

3.2 Transfer matrix eigenvalues

In the previous subsection we illustrated how branch resonance results in total reflection and a motionless string beyond the resonant junction. We continue by attempting to add further insight into the character of solutions along the string through the consideration of transfer matrix eigenvalues.

The scattering across an array of N branches is determined by the product of the N transfer matrices Q_n. The eigenvalues of the transfer matrix encode characteristics of how the solution communicates from one junction to the next.

Since the determinant of the transfer matrix Q_n is unity, eigenvalues are found in reciprocal pairs and are found as

$$\lambda_n = \sigma_n \pm \sqrt{\sigma_n^2 - 1} \quad (\equiv \sigma_n \pm \mathrm{i}\sqrt{1-\sigma_n^2}) \tag{30}$$

where $\sigma_n = \cos k(c_n + \delta_n)/\cos kc_n$ and $d\sigma_n/dk < 0$ for $k\delta_n < \pi$.

As $k \to 0$, $\sigma_n \to 1^-$, a value from which σ_n decreases as k increases towards $\frac{1}{2}\pi/c_n$. The rate of decrease of σ_n is rapid over $\frac{1}{2}\pi/(\delta_n + c_n) < k < \frac{1}{2}\pi/c_n$. Thus when $k = \frac{1}{2}\pi/(\delta_n + c_n)$, $\sigma_n = 0$ and $\sigma_n \to -\infty$ as $k \to \frac{1}{2}\pi/c_n$ from below, passing through -1 in the narrow range of values of k between $\frac{1}{2}\pi/(\delta_n + c_n)$ and $\frac{1}{2}\pi/c_n$. For values of k just above $\frac{1}{2}\pi/c_n$, σ_n is large and positive and as k increases further towards π/c_n σ_n decreases towards 1 from above.

The eigenvalue trajectory as a function of increasing k follows from the relationship between λ_n and σ_n in (30). Thus, as k increases from zero eigenvalues move around the unit circle from 1 in complex conjugate pairs, slowly at first and then rapidly to -1 on the real axis and, even more rapidly, along the real axis in reciprocal pairs, one towards $-\infty$ and reappearing at $+\infty$ across $k = \frac{1}{2}\pi/c_n$, the other towards and through zero on the real axis.

Complex conjugate eigenvalues on the unit circle are characteristic of wave-like behaviour whilst eigenvalues on the real axis are characteristic of exponential behaviour. For example, in Fig. 8, $kc_n < \frac{1}{2}\pi$ for all n in the array and the plot of $|D_n|$ shows oscillatory behaviour across the array. In Fig. 9 $kc_n > \frac{1}{2}\pi$ for all n in the array and the plot of $|D_n|$ shows exponential decay. In the most complicated case, in Fig. 10, the central 51st string in an array of 101 branches of tapered length is tuned to resonance. Thus, $kc_{51} = \frac{1}{2}\pi$, $kc_n < \frac{1}{2}\pi$ for $n < 51$ and $kc_n > \frac{1}{2}\pi$ for $n > 51$. We have already established (analytically) that $D_n = 0$ for $n > 51$ which is confirmed numerically in Fig. 10. We also note oscillations prior to $n = 51$ and a sharp increase in $|D_n|$ for n very close to 51. Thus, the eigenvalues of the transfer matrix provide some information on the behaviour of the solution.

3.3 A continuum limit ?

Instead of the variables β_n and γ_n, consider the transformation

$$\Gamma_n = \beta_n + \gamma_n^*, \qquad \Upsilon_n = \mathrm{i}(\beta_n - \gamma_n^*) \tag{31}$$

and then the pair of recurrence relations defined in terms of β_n and γ_n are transformed into

$$\Gamma_n = \cos k\delta_n \Gamma_{n-1} + \sin k\delta_n \Upsilon_{n-1} \tag{32}$$

$$\Upsilon_n = (\cos k\delta_n - 2t_n \sin k\delta_n)\Upsilon_{n-1} - (2t_n \cos k\delta_n + \sin k\delta_n)\Gamma_{n-1} \tag{33}$$

with $\Gamma_1 = \mathrm{e}^{\mathrm{i}k\delta_1}$ and $\Upsilon_1 = (\mathrm{i} - 2t_1)\mathrm{e}^{\mathrm{i}k\delta_1}$.

The amplitudes along each branch are characterised by the coefficient D_n which, under the current variables, may be expressed as

$$D_n = \sec kc_n(\Gamma_n + R\Gamma_n^*) \tag{34}$$

assuming R has been found from

$$R = -(\Gamma_N + \mathrm{i}\Upsilon_N)/(\Gamma_N^* + \mathrm{i}\Upsilon_N^*). \tag{35}$$

Let the branch separation $\delta_n = \delta$ be identical and assume $k\delta \ll 1$. Then the pair of discrete equations are, to first order in $k\delta$, approximately

$$\Gamma_n \approx \Gamma_{n-1} + k\delta\Upsilon_{n-1} \tag{36}$$

$$\Upsilon_n \approx \Upsilon_{n-1} - 2t_n\Gamma_{n-1}. \tag{37}$$

Since $x_n = n\delta$ we suppose that $\Gamma_n = \Gamma(x_n)$, $\Upsilon_n = \Upsilon(x_n)$ and $c_n = c(x_n)$, $n = 1, 2, \dots N$ are discrete evaluations of continuous functions. The equations above may be intepreted as discrete approximations to the coupled first order system of ODEs

$$\Gamma'(x) = k\Upsilon(x), \qquad \Upsilon'(x) = (-2/\delta)\tan(kc(x))\Gamma(x) \tag{38}$$

or

$$\Gamma''(x) = -2(k/\delta)\tan(kc(x))\Gamma(x), \qquad 0 < x < L \tag{39}$$

with $\Gamma(0) = 1$, $\Gamma'(0) = k(\mathrm{i} - 2\tan(kc(0)))$. Evidently, letting $\delta \to 0$ does not result in a continuum limit being reached.

However, (39) with $k\delta \ll 1$ is a classical problem to which the WKB approximation can be applied (see, for example, Bender & Orszag (1978)) to give

$$\begin{aligned}\Gamma(x) \approx [2k\tan(kc(x))]^{-1/4}\Bigg\{ & C_+\exp\left(\mathrm{i}\sqrt{\frac{2k}{\delta}}\int_0^x \tan^{1/2}(kc(s))\,ds\right) \\ & + C_-\exp\left(-\mathrm{i}\sqrt{\frac{2k}{\delta}}\int_0^x \tan^{1/2}(kc(s))\,ds\right)\Bigg\}\end{aligned} \tag{40}$$

where $C_\pm = \frac{1}{2}(A \pm B)$ and $A = [2k\tan(kc(0))]^{1/4}$, $B = -\mathrm{i}\sqrt{\delta}[2k\tan(kc(0))]^{-1/4}(\mathrm{i} - 2\tan(kc(0)))$.

For certain choices of $c(x)$ such as $c(x) = a + bx$, the integral under the exponential can be performed analytically, although the result is algebraically complicated.

We note that $D(x)$, the continuous variable approximation to D_n, is given by $D(x) = \sec(kc(x))(\Gamma(x) + R\Gamma^*(x))$. If $kc(x) < \frac{1}{2}\pi$ for all $0 < x < L$ then the exponentials in (39) are oscillatory and hence we predict $D(x)$ to be oscillatory (e.g. Fig. 8). If $kc(x) > \frac{1}{2}\pi$ for all $0 < x < L$ then the arguments of the exponentials in (39) are real and we expect exponential behaviour in $D(x)$ (as in Fig. 9). If $kc(x) < \frac{1}{2}\pi$ for $0 < x < x^*$ with $kc(x^*) = \frac{1}{2}\pi$ (x^* can be less than or greater than L) the oscillatory nature of the exponentials in (40) allows us to predict that

$$|D(x)| \sim C\sec^{3/4}(kc(x)), \qquad \text{as } x \to x^* \text{ from below} \tag{41}$$

for some constant C. In other words

$$|D(x)| \sim \frac{C}{[kc'(x^*)(x^* - x)]^{3/4}}, \qquad \text{as } x \to x^* \text{ from below} \tag{42}$$

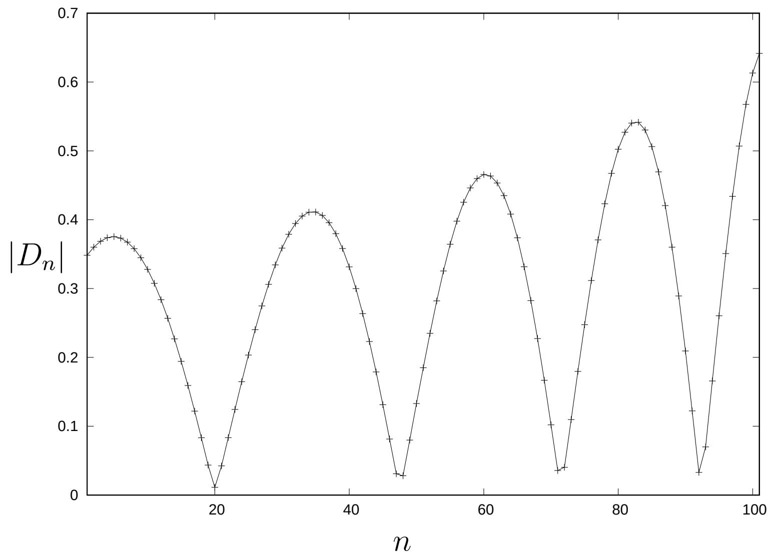

Figure 8: Modulus of amplitude on branch n against n for $N = 101$ branches at $c_n = 1 + \delta(n - 51)$, $\delta = 0.005$ and $k = 1$.

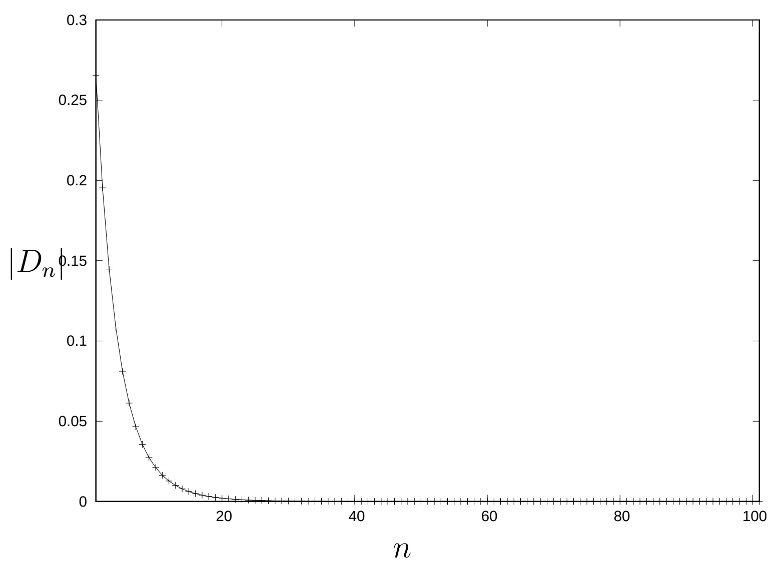

Figure 9: Modulus of amplitude on branch n against n for $N = 101$ branches at $c_n = 1 + \delta(n - 51)$, $\delta = 0.005$ and $k = 2.5$.

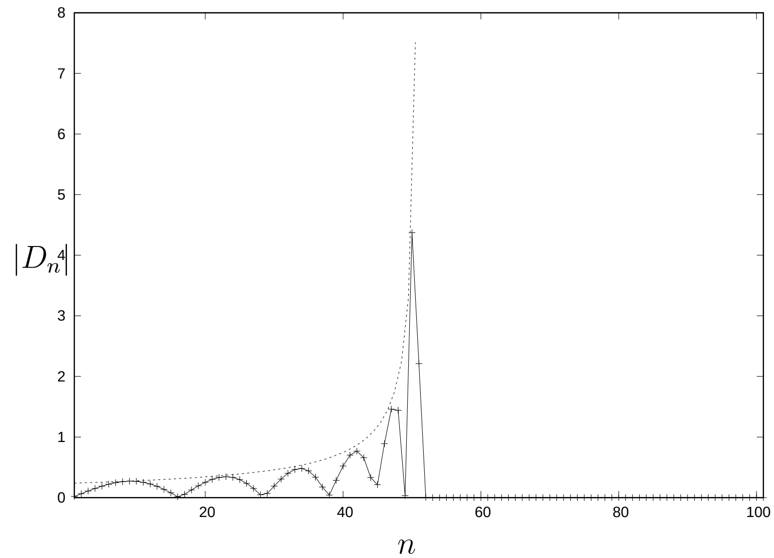

Figure 10: Modulus of amplitude on branch n against n for $N = 101$ branches at $c_n = 1+\delta(n-51)$, $\delta = 0.005$ and $k = \pi/2$. The dotted envelope is defined by the line $\pm 4.5/(51-n)^{3/4}$.

For example, in Figs. 10–12 we have taken $c(x) = 1 + (x - L/2)$ and $k = \frac{1}{2}\pi$ so that $x^* = L/2$. In terms of discrete variables, (42) is written $D_n \sim (2C/\pi)/(\frac{1}{2}N - n)^{3/4}$ as $n \to \frac{1}{2}N$ from below. There is excellent agreement between the computations and this predicted behaviour as shown by the dotted curves added to Figs. 10–12.

Figs. 11 and 12 plot a snapshot in time of displacement along $N = 201$ side branches against branch number, n, for two values of $\delta \ll 1$ which differ by a factor of ten. The plots are very similar and suggestive of convergence as $\delta \to 0$, despite earlier remarks made on the absense of a continuum limit. In fact this is an isolated example of convergence as $\delta \to 0$ which holds for the particular definition of $c(x) = 1 + (x - \delta N/2)$, $L = \delta N$ and for the specific value of $k = \frac{1}{2}\pi$ chosen. Application of a rescaling $x = \delta X$ (integer values of X coincide with branch number), $\hat{\Gamma}(X) \equiv \Gamma(x)$ to (39) gives, after making a leading order approximation to the function $\tan(x)$ near $x = \frac{1}{2}\pi$,

$$\hat{\Gamma}''(X) \approx \frac{2\hat{\Gamma}(X)}{X - \frac{1}{2}N}, \qquad 0 < X < N \tag{43}$$

with $\hat{\Gamma}(0) = 1$, $\hat{\Gamma}'(0) = O(\delta) \approx 0$ assuming $\delta \ll 1$. In fact (43) with the initial conditions stated has the explicit solution

$$\hat{\Gamma}(X) = \pi\sqrt{N - 2X}\left\{Y_0(2\sqrt{N})J_1(2\sqrt{N - 2X}) - J_0(2\sqrt{N})Y_1(2\sqrt{N - 2X})\right\} \tag{44}$$

for $0 < X < N$, expressed in terms of Bessel functions. The function $\hat{\Gamma}$ is only indirectly related to R and the amplitudes along the branches. In Fig. 13 we plot a comparison between Γ_n for a discrete system and $\hat{\Gamma}(X)$ from (44) with $N = 200$ from the analogous continuous solution for the first half of the junctions where the solutions are oscillatory in the case described in Fig. 12.

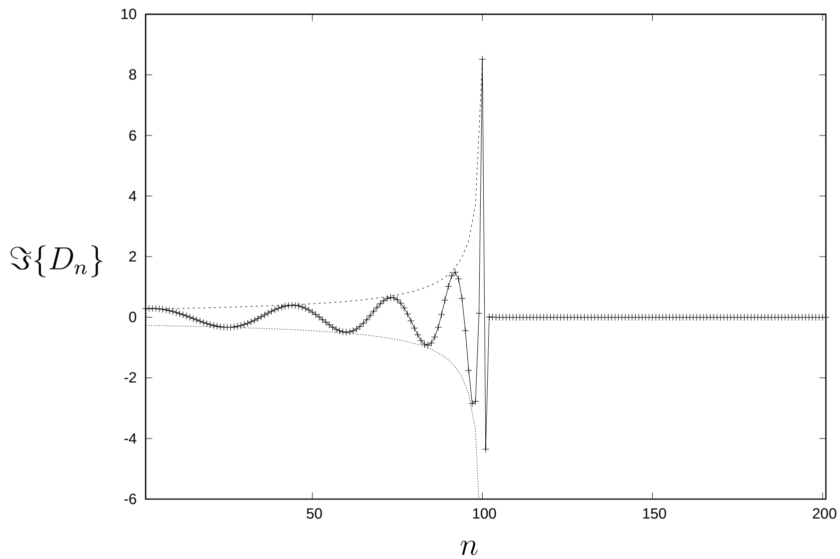

Figure 11: Modulus of amplitude on branch n against n for $N = 201$ branches at $c_n = 1+\delta(n-101)$, $\delta = 0.01$ and $k = \pi/2$. The dotted envelope is given by the lines $\pm 8.5/(101-n)^{3/4}$.

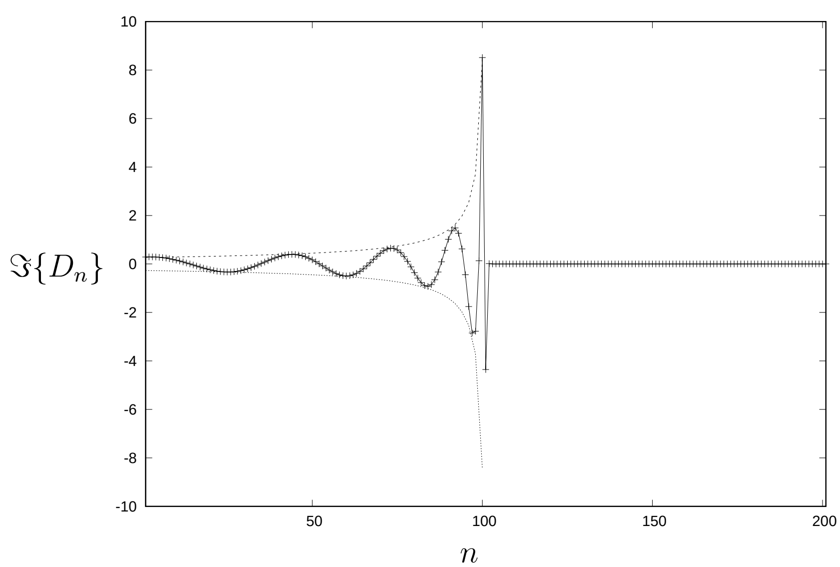

Figure 12: Modulus of amplitude on branch n against n for $N = 201$ branches at $c_n = 1+\delta(n-101)$, $\delta = 0.001$ and $k = \pi/2$. The dotted envelope is given by the lines $\pm 8.5/(101-n)^{3/4}$.

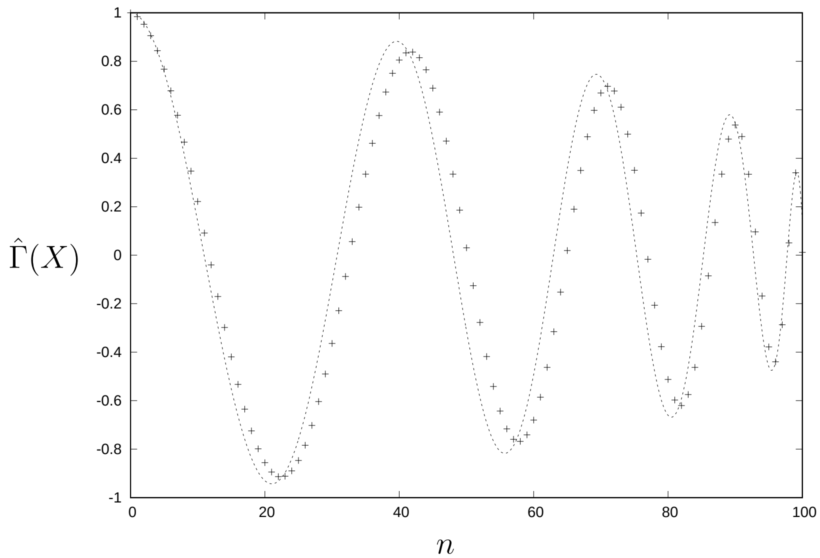

Figure 13: Comparison of Γ_n, $n = 1, 2, \ldots, 101$ (crosses, plotted against $n - 1$) to $\hat{\Gamma}(X)$, $0 < X < 100$ for the arrangement in Fig. 12.

4 Conclusions

We have consider the effect of a finite number (N) of finite length strings which are tied perpendicularly across an infinitely-long string on the propagation of waves along that string. The solution has been described simply in terms of 2×2 scattering and transfer matrices which propagate information along the string from one branch to the next.

We have shown that for frequencies when any of the branched strings is resonant there is total wave reflection and that the string beyond the resonant branch is rendered motionless. This has been used to demonstrate how an array of branched strings of tapered length can be used to construct a broadbanded stop filter on the main string.

We have also considered the limit where N is large and an equal separation (δ) between neighbouring strings is small. It has been shown that discrete equations describing the scattering process can be approximated by an ODE and the solution to that ODE can be approximated by the WKB method. This allows use to determine the behaviour of the amplitudes on, for example, the nth string on a linearly-tapered array prior to the resonant string (n^*, say). Hence amplitudes grow like $O((n^* - n)^{-3/4})$ as $n \to n^*$ from below (and are exactly zero beyond $n = n^*$).

It is possible this behaviour is characteristic of other situations where 'rainbow trapping' by linearly-tapered arrays occurs (Jan & Porter (2018)) and that the behaviour can be used to help develop numerical solutions to those problems.

References

1 Jan, A. & Porter, R. (2018) Acoustic wave transmission along a waveguide with a metamaterial cavity. *In submission to J. Acoust. Soc. Am.*

2 Bender, C. & Orszag, S. (1978). *Advanced Mathematical Methods for Scientists and Engineers.* McGraw-Hill.